13th World Conference on Earthquake Engineering
Vancouver, B.C., Canada
August 1-6, 2004
Paper No. 2468

STRUCTURAL PERFORMANCE OF RC COLUMNS USING DOUBLE RIGTH ANGLE ANCHORAGE HOOPS WITH HIGH STRENGTH BARS

Juan Jose CASTRO[1], Hiroshi IMAI [2]

SUMMARY

The purpose of this research is to verify the seismic behavior of columns elements reinforced with the new proposed double right angle anchor (double anchorage) type hoops, comparing them with the conventional welded closed type hoops by using supper high strength reinforcing bars.

Twenty-two column specimens were tested under simulated seismic actions. The variables for this study were the concrete strength (24, 36, 45, 60 N/mm^2), transverse reinforcement ratio (0.16, 0.21, 0.27, 0.36, 0.40, 0.60%), failure type (bending, shear), hoop type (welded hoop, double anchorage hoop), the anchor length of the hook (6d, 12d, 15d, 24d), and the axial force ratio (0.15, 0.25%). The column specimens were subjected to cyclic anti-symmetrical bending moments under constant axial forces.

Test results showed that, when the anchor length of the hook is longer than 15d, enough anchorage strength can be attained and the seismic behavior of specimens reinforced with double anchorage hoops is comparable with those specimens reinforced by welded closed type hoops.

INTRODUCTION

The use of super high strength steel bars (σ_y=1275 N/mm^2) and high strength concrete has gained popularity over the recent years in Japan because of the tall building construction demand. For the columns of these tall buildings, in order to give enough confinement to the main bars and core concrete, it is necessary to place peripheral hoops enclosing all the longitudinal bars together with inner ties or inner hoops as lateral reinforcement. Moreover, in order to meet the high shear strength demand of high-rise buildings, super high strength steel is being used extensively as lateral reinforcement.

Using super high strength steel bars with the conventional 135° hook method, like the shown in Fig. 1, the development length (anchor length) required by the Japanese standards [1], [2] is extended from the 6d (d: bar diameter) for conventional bars, to 8d or even to 10d in some cases. Moreover in case of high-rise buildings, it is always required the use of inner hoops due to the high shear stresses acting on the columns.

[1] Senior Researcher, Kabuki Construction Co. Ltd., Tokyo, Japan. Email: castro.j@kabuki.co.jp
[2] Professor, University of Tsukuba, Ibaraki, Japan. Email:imai@kz.tsukuba.ac.jp

Then when dense transverse reinforcement is placed, the straight extension beyond the hooks (anchor hook) interfere with the concrete placing and its proper compaction by mean of vibrators at the construction site.

When welded closed type hoops are used as lateral reinforcement, it is possible to place dense reinforcement avoiding the problem of poor anchorage of hooks and improper concrete compaction. However, the severe quality control needed due to the poor weldability of super high strength bars, remains as a week point of this type of hoops.

The method of hoops with double right angle hook anchorage (so-called here double anchorage type hoops) shown in Fig. 2 was proposed [3] as a solution to these problems. Using this method, welding becomes unnecessary, improving the workability of the bar arrangement and the concrete placing at the construction site.

The aim of this research is to examine the behavior during a simulated major earthquake loading of column specimens reinforced with double anchored type hoops by using supper high strength reinforcing bars, provided with several types of anchorage lengths. The test results were compared with those obtained for specimens reinforced with the conventional welded closed type hoops.

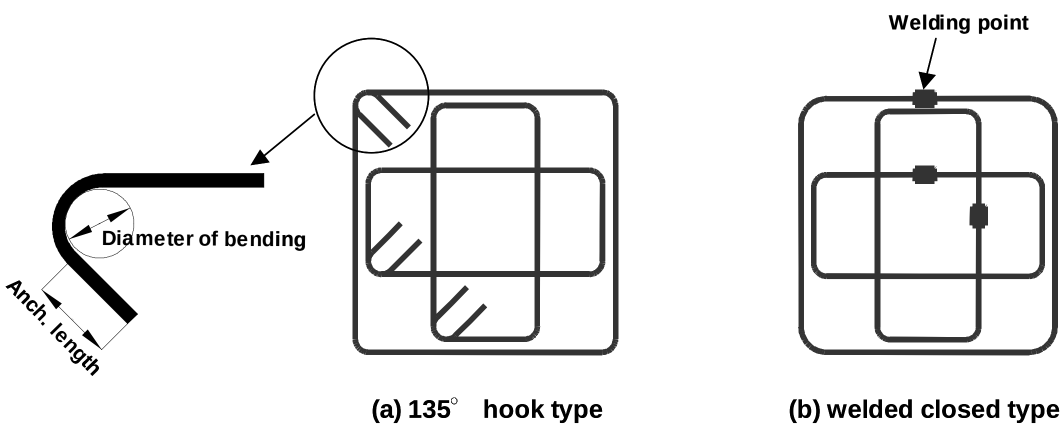

Fig. 1 Conventional hoops

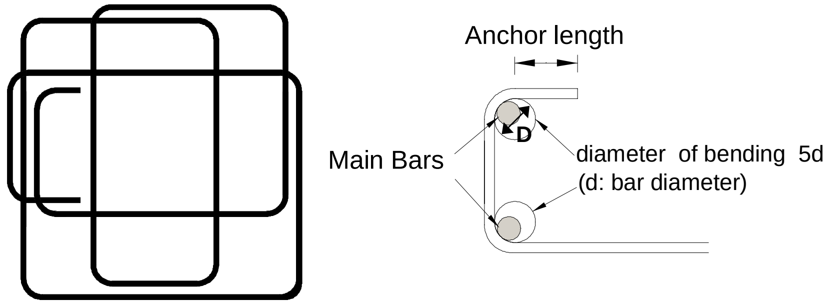

Fig. 2 Detail of double anchorage type hoops

EXPERIMENTAL PROGRAM

Specimens Outline and Materials

The features of the test specimens are listed in Table 1 and their geometries are shown in Fig. 3. A total of 22 specimens were tested. Five of them were designed to have bending failure type, and the other 17 to have either shear failure type or bond splitting failure type. Since these two types of failure are in fact very close, they will be referred as shear failure type in the discussion of the test results.

Table 1 Summary of the test specimens

Spec.	Failure Mode	M/QD	Main Bars		Lateral reinforcement			Fc	η
			Grade	Number (P_g)	Diameter (pitch)	p_w	Anchorage Type (length)		
C3W	BFT	2	SD345	12-D19 (1.70)	4-U7.1 (@100)	0.36	WCT	24	0.15
C3SS							40 mm (6d)		
C3M							100 mm (15d)		
C4W	SFT	1.5	SD645	12-D19 (1.70)	4-U7.1 (@170)	0.21	WCT	24	
C4SS							40 mm (6d)		
C4M							100 mm (15d)		
C9W	BFT	2	SD345	12-D22 (2.29)	4-U6.4 (@100)	0.27	WCT	45	
C9M							100 mm (15d)		
C10W	SFT	1.5	SD685	12-D22 (2.29)	4-U6.4 (@170)	0.16	WCT	36	
C10M							100 mm (15d)		
C10L							150 mm (24d)		
C11W							WCT	45	
C11M							100 mm (15d)		
C11L							150 mm (24d)		
C12W	SFT	1.5	USD1080	12-D22 (2.29)	4-U7.1 (@140)	0.25	WCT	60 (80)	0.25 (0.19)
C12M							106 mm (15d)		
C13W					4-U7.1 (@90)	0.40	WCT		
C13M							106 mm (15d)		
C14W					4-U7.1 (@60)	0.60	WCT		
C14M							106 mm (15d)		
C14S							85mm (12d)		
C14R90							106 mm (15d)		

WCT: welded closed type; S, M, L: length of anchor (**S**hort, **M**iddle, **L**ong)
BFT: Bending Failure Type; SFT: Shear Failure Type
Fc: Specified concrete strength (N/mm^2)
p_g: longitudinal reinforcement ratio (%) ; p_w: lateral reinforcement ratio (%)
η=N/(bDFc) : Axial force ratio ( ) indicates the actual values

The column height was 1350 mm for the shear failure type, and 1800 mm for the bending failure type, with a common section for all specimens of 450 x 450 mm. The specimens were designed using four types of concrete strength, 24, 36, 45 and 60N/mm^2, respectively. For the lateral reinforcement, super high strength USD1275/1420 (specified yield strength σ_y= 1275 MPa) deformed steel bars were used.

The specimens with double anchorage type hoops, presented variations on the hook anchorage lengths of 6d (40mm), 12d (85mm), 15d (100mm, 106mm) and 24d (50 mm), where d represents the bar diameter of the hoops. Considering the most critical case, in principle the double anchorage hook parts were placed in the loading direction. However, in case of specimen C14R90, in order to be able to compare, the position of the double anchorage was rotated 90 degrees.

For main bars, high strength steel bars of SD685 (specified yield strength of 685 MPa) and USD1080/1225 (specified yield strength of 1080 MPa) were used for the shear failure type, and normal grade bars of SD345 (specified yield strength of 345 MPa) for the bending failure type. For specimens C12, C13 and C14, the specified concrete was 60N/mm^2, but the actual strengths varied from 78 to 81 N/mm^2. In this case the design axial force ratio (η=N/ bDFc) was to be 0.25, but it was changed to 0.19 because of the impossibility of increase the axial load due to the capacity of the loading system. The actual mechanical characteristics of the materials are listed in Table 2 and Table 3.

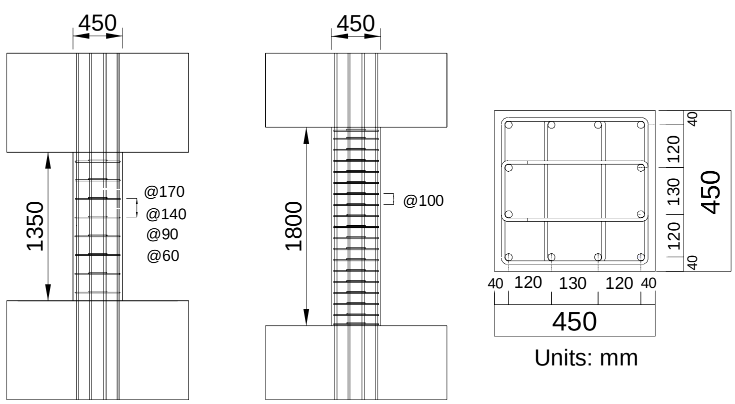

(a) Shear Failure (b) Bending Failure (c) Column Section

Fig. 3 Typical specimen

Table 2 Mechanical Properties of Steel bars

Size	Grade	σ_y N/mm^2	σ_t N/mm^2	Comments
D19	SD345	401	562	C3 (main bars)
D19	SD685	732	946	C4 (main bars)
U7.1	USD1275	1448	1479	C3, C4 (hoops)
D22	SD345	400	527	C9 (main bars)
D22	SD685	722	930	C10～C11 (main bars)
U6.4	USD1275	1516	1537	C9, 10, 11 (hoops)
D22	USD1080	1150	1262	C12, C13, C14 (main bars)
U7.1	USD1275	1444	1483	C12, C13, C14 (hoops)

σ_y: Yielding Strength, σ_t: Tensile Strength

Table 3 Mechanical Properties of Concrete

Specimens	Fc N/mm^2	σ_B N/mm^2	σ_t N/mm^2	E kN/mm^2
C3	24	26.6	2.3	27.2
C4	24	24.4	2.6	23.8
C9	45	39.7	2.9	22.8
C10	36	33.9	2.8	24.2
C11	45	41.5	3.0	25.1
C12	60	80.6	5.1	36.7
C13	60	79.9	6.1	35.0
C14	60	78.0	6.1	35.1

σ_B: Compressive Strength, σ_t: Splitting Strength
E: Young's Modulus

Loading System

Each specimen was set under the loading apparatus as shown in Fig. 4. The specimens were subjected to varying shear forces that were applied cyclically to produce anti-symmetric bending moment distribution while being acted upon by a constant axial load.

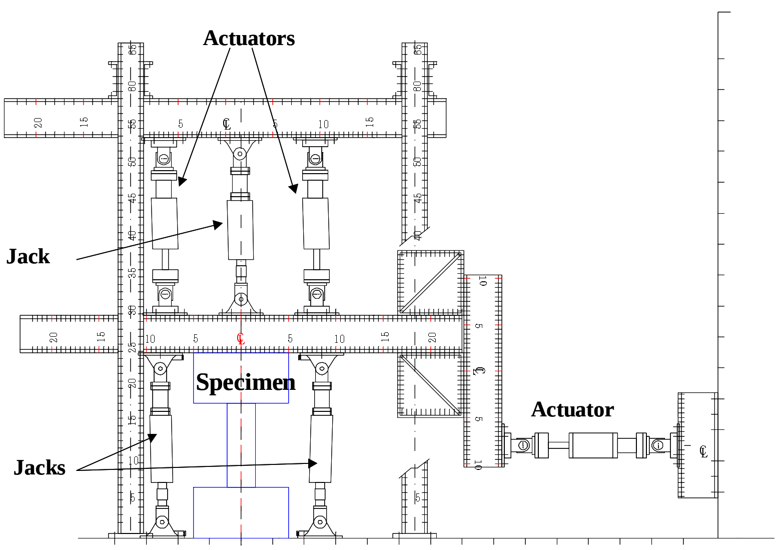

Fig. 4 Loading System

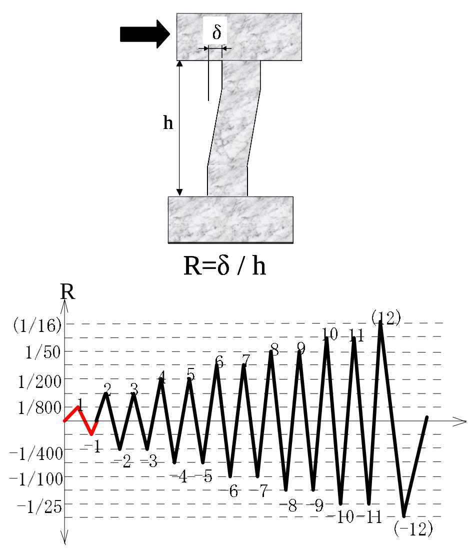

Fig. 5 Loading History

For specimens with shear failure type the applied loading history was once at R=1/800, then twice at 1/400, 1/200, 1/100, 1/50, 1/25. On the other hand, for specimens with bending failure type the loading was furthermore extended once to R=1/16, as shown in Fig. 5. The loading history was controlled in terms of lateral drift angle. The lateral drift angle R is defined as the relative displacement (δ) between the lower and upper stubs divided by height (h) of the test portion (R=δ / h).

TEST RESULTS

Crack Pattern

The crack patterns for representative specimens with bending failure and shear failure type are shown in Fig. 6 (a) and (b), respectively. For specimens with bending failure, the initial flexural cracks were observed at the column ends when the drift angle was R=1/800. The cracks tended to incline at R=1/200 becoming flexure-shear cracks. At R=1/200, after the main bars yielded the cracks developed wider. Finally, at R=1/25 crashing of concrete at the column compression side was observed, following concrete spalling off.

For shear failure type specimens, the initial cracks appeared on both ends of the column at R=1/800. The shear cracks started to be noticeable at R=1/200 on the middle part of the column, then at R=1/100 a severe shear crack appeared along the column specimens between the top and bottom stubs. At R=1/50, bond splitting cracks appeared along the first layer of the main bars, following by concrete cover spalling off. In general, no differences were observed between the specimens with welded closed type hoops and those with the double anchorage type hoops

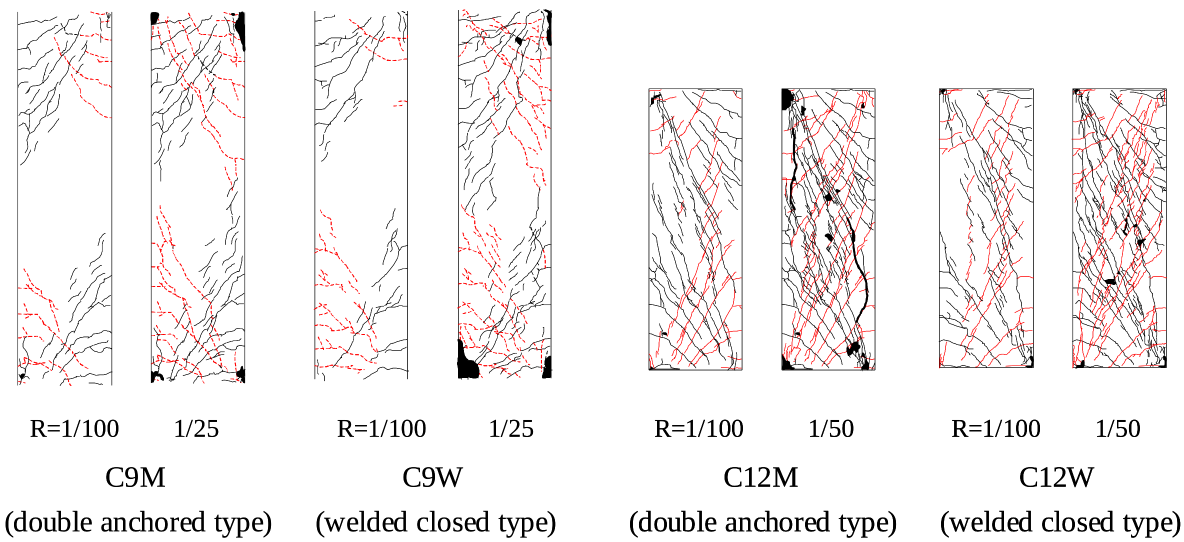

(a) Bending failure type (b) Shear failure type

Fig. 6 Crack Pattern

Load Displacement Relationships

The hysteresis curves are shown in Fig. 7. For comparison the theoretical values are plotted in these figures. The bending strength (Q_{mu}) was calculated in terms of shear force, by the equation given by the Building Center of Japan (BCJ) [4], the shear strength (Q_{su}) was calculated by the equation given by the so called Method A of the Architectural Institute of Japan (AIJ) [5] and the bond strength was calculated by Kaku's Equation [6]. For bending and shear failure type specimens the experimental values of the maximum strength, correspond very well with the values calculated by the equations indicated above.

For specimens C3 with bending failure type, the Fig. 7(a) shows that the hysteresis curves of specimens are very similar independently of the type of hoops they were provided with. Even among the specimens with double anchorage hoops they presented similar patterns in spite of the variations of the anchor lengths.

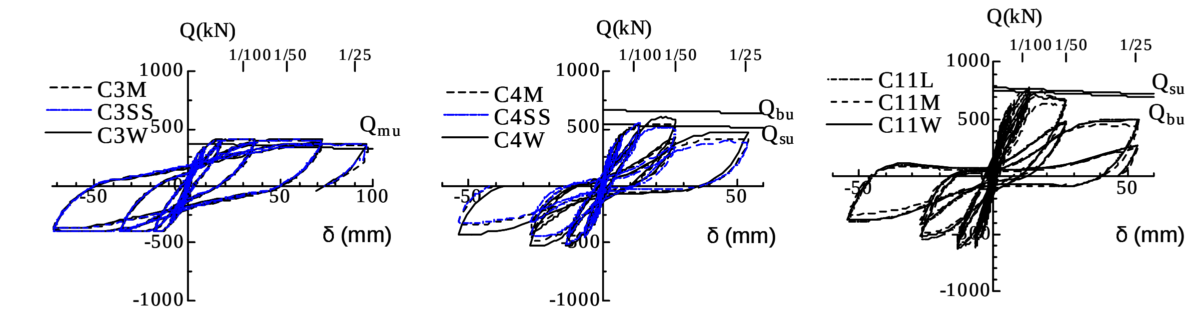

(a) Fc=24 N/mm^2, p_w=0.36%, η=0.15 (b) Fc=24 N/mm^2, p_w=0.21%, η=0.15 (c) Fc=45 N/mm^2, p_w=0.16%, η=0.15

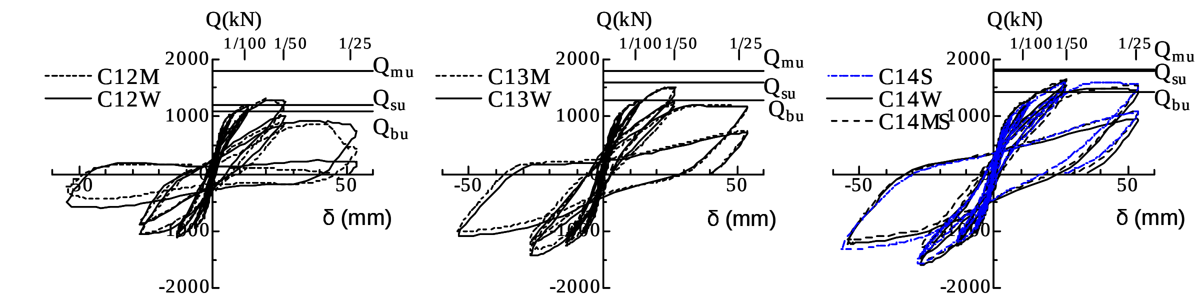

(d) Fc=60 N/mm^2, p_w=0.25%, η=0.19 (e) Fc=60 N/mm^2, p_w=0.4%, η=0.19 (f) Fc=60 N/mm^2, p_w=0.6%, η=0.19

Fig. 7 Load Displacement Relationships

Specimens C4SS and C4M (Fc=24N/mm^2) with shear failure type, showed a decrease of 10% on their ultimate shear strength compared to the specimen with welded closed type hoops (C4W) as shown in Fig. 7 (b). This can be attributed to the loose of adherence of the end part (anchor hook) of the double anchorage hoops due to concrete failure, indicating that the provided anchor length does not give enough anchor strength. However, for specimens with Fc=36N/mm^2 or greater, no differences were observed in spite of the different anchorage methods used for the lateral reinforcement. Similar hysteresis curves were observed for specimens C14S and C14W, indicating that an anchorage length (hook length) of 12d or greater, provide enough anchor strength at the anchor part.

Envelope Curves

The envelope curves of the hysteretic loops corresponding to the shear failure type specimens are shown in Fig. 8. Among the specimens with concrete strength of Fc=24N//mm^2, those reinforced with double anchorage hoops (C4M, C4SS), showed lower maximum strength compared with the specimens reinforced with welded closed type hoops. For specimen C4W with welded closed type hoops the maximum strength was reached at R=1/50, while for C4SS and C4M, which were reinforced with double anchorage hoops, the maximum strength was reached at R=1/100.

In case of Specimen C4SS with short anchorage length, 40mm (6d), after reaching its maximum strength showed pronounced strength decay, as a consequence of the poor anchorage of the anchor hooks. On the other hand, specimens with concrete strength of 36N/mm^2 or greater presented similar envelope curves, independently of the types of hoops used as lateral reinforcement, as shown in Fig. 8 (b).

The envelope curves, for specimens with different concrete strength under the same axial force ratio (η=0.15), are shown in Fig. 8 (c). As the concrete strength is increased, the ultimate shear strength also increased. However, after reaching the peak pronounced strength decay was observed. At large deformations the shear strength becomes comparable with that obtained for the specimens with lower concrete strength. This can be attributed to the fact that relatively small lateral reinforcement ratio (p_w) was used for these specimens, thus they lost their capacity of deformation at large lateral drift angles.

Concerning to specimens with axial force ratio of η=0.19 (Fc=60N/mm^2), when the lateral reinforcement ratio (p_w) is increased, the maximum strength also increase as shown in Fig. 8 (d). Also with higher p_w it is possible to control the loose of strength after the peak was attained.

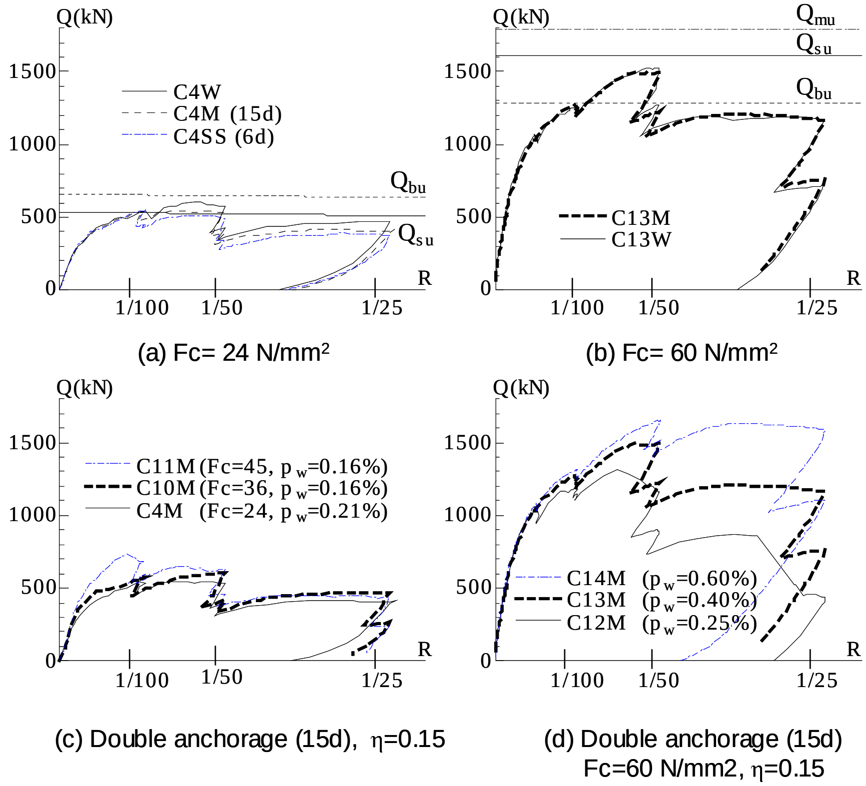

Fig. 8 Envelope Curves

Ultimate Shear Strength

The bending strength (Q_{mu}), shear strength (Q_{su}), bond strength (Q_{bu}), and the experimental values are shown in Table 4. Specimens with bending failure type (C3, C9) showed experimental values greater that the calculated ones and no differences were observed regardless of the anchorage method and anchor lengths variations.

Among the specimens with shear failure type, for those with concrete Fc=24, 36 and 45N/mm^2, the experimental values are compared with their shear strengths. In all cases the experimental values are greater than the calculated ones. In the case of specimens with Fc=60N/mm^2, since the lower strengths were the bond splitting strengths, they were compared with the experimental values.

In case of specimens C4 with Fc=24N/mm^2, it can be appreciated some differences (up to 10%) of the strengths ratio between welded closed type (1.14) and the double anchored type (1.02, 1.04). However, for the rest of specimens no differences are recognized in spite of the different anchorage methods for lateral reinforcement.

Table 4 Experimental and Calculated Shear Strengths

Spec.	Failure Mode	Shear Strength Q_{su}	Bond Splitting Strength Q_{bu}	Bending Strength Q_{mu}	Actual Strength Q_{exp}	Q_{exp}/Q_{cal}
C3W	BFT	774	711	376	431	1.15
C3M		866	770	378	430	1.14
C3SS		856	844	378	426	1.13
C4W	SFT	545	741	745	620	1.14
C4M		541	738	745	553	1.02
C4SS		536	663	746	556	1.04
C9W	BFT	971	784	579	605	1.04
C9M		956	778	578	604	1.04
C10W	SFT	577	663	1021	646	1.12
C10L		602	689	1024	654	1.09
C10M		572	683	1021	626	1.09
C11W		710	708	1098	789	1.11
C11L		669	702	1093	768	1.15
C11M		702	707	1097	750	1.07
C12W	SFT	1328	1178	1959	1300	1.10
C12M		1328	1178	1959	1320	1.12
C13W		1683	1286	1959	1520	1.18
C13M		1691	1281	1956	1500	1.17
C14W		1891	1425	1956	1640	1.15
C14M		1891	1425	1956	1650	1.16
C14S		1902	1416	1893	1610	1.14
C14R90		1902	1416	1923	1620	1.14
C14MS		1902	1416	1951	1640	1.16
Units: kN						

Bond Stresses

The influence of the anchorage method of the hoops on the bond stresses of main bars for shear failure type specimens is studied in this section. For specimens with double anchored type hoops, the main bars are divided in those located in the anchored side and those located in the non-anchored side as shown in Fig. 9. Because the main bars did not yield (they always remained in the elastic range), the stresses can be calculated based on the measured strains as shown in Fig. 10, using the Eq. (1).

$$\tau = \frac{a\,E\Delta\varepsilon}{\phi\,L} = \frac{a\,E}{\phi}\frac{\Delta\varepsilon}{L} = \frac{a\,E}{\phi}\alpha \qquad (1)$$

a: area of main bars
E: Young's coefficient

Φ: perimeter of main bars
$\Delta\varepsilon$: Difference of strain between strain gauges at main bars
α: slope of the main bar strain distribution
L: bond length (here only the 60% of the column height (central portion) is considered as bond length)

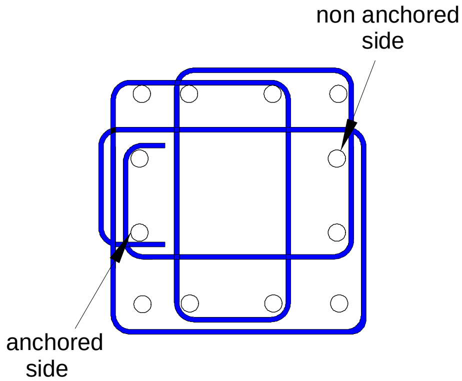

Fig. 9 Main bars location

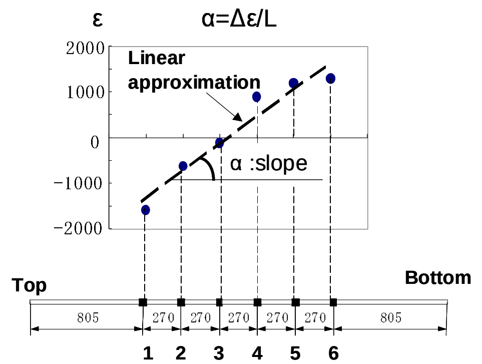

Fig. 10 Method of Calculation of α

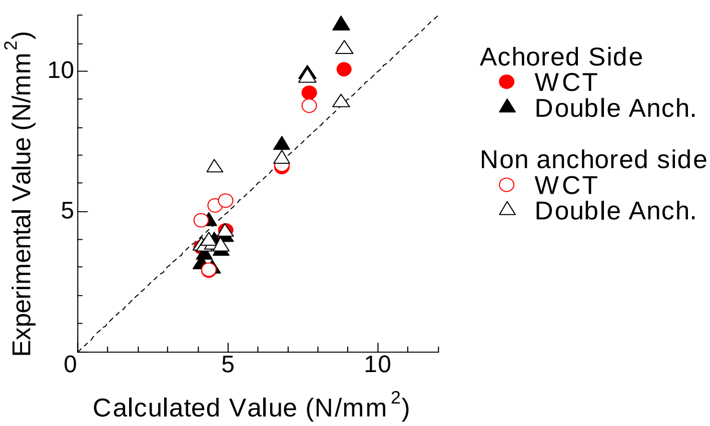

Fig. 11 Comparison of the main bars bond stress

The comparison between the experimental and the calculated values of the bond stresses is shown in Fig. 11. The calculated values were obtained using Kaku's Equation [6].

No differences were observed among bars located at the anchored side and those located in the non-anchored side. Hence it is possible to understand that there is no influence of the lateral reinforcement anchors on the main bars bond stresses. Also, the comparison of the bond stresses showed a good correspondence with the specimens with welded closed type hoops

Strain Development of the Lateral Reinforcement

(a) Strain at Center of the Column

For specimens with bending failure type the strain gauges were located in two layers at each end of the column. On the other hand for specimens with shear failure type they were located in four layers at the middle height of the column. The strain distributions of lateral reinforcements for all specimens are shown in Fig. 12. The strain values plotted in the figure represent the average values of all strain gauges placed for each specimen.

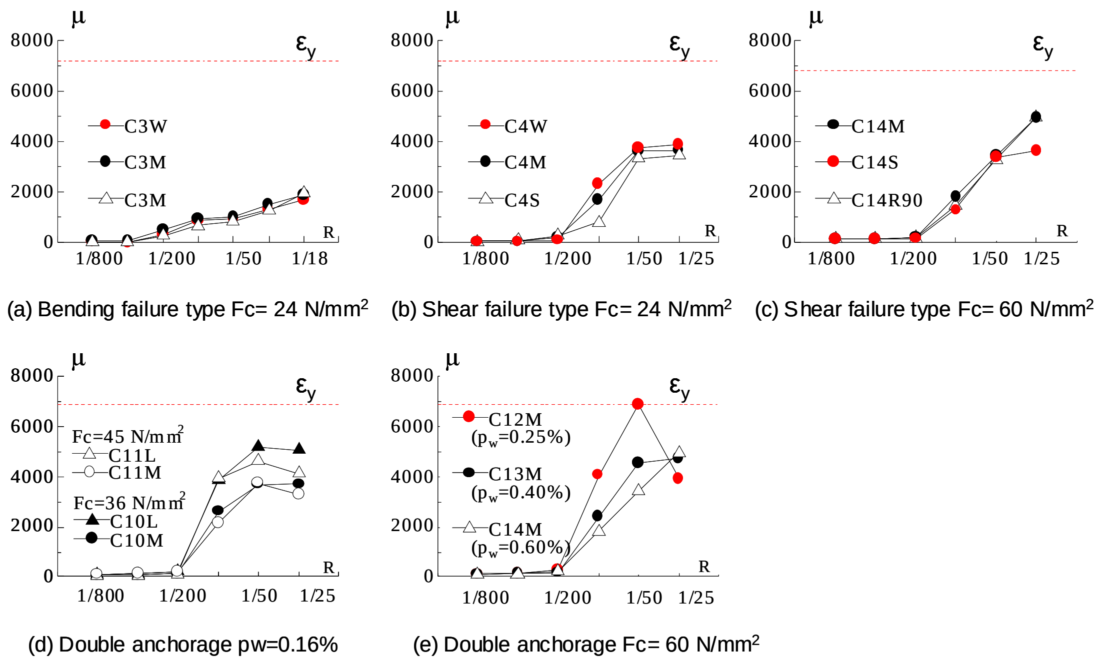

(a) Bending failure type Fc= 24 N/mm^2 (b) Shear failure type Fc= 24 N/mm^2 (c) Shear failure type Fc= 60 N/mm^2

(d) Double anchorage pw=0.16% (e) Double anchorage Fc= 60 N/mm^2

Fig. 12 Strain development of lateral reinforcement

Until R=1/18 bending failure type specimens, independently they were reinforced with welded closed type hoops or double anchorage type hoops, showed similar strain development along the loading history as shown in Fig. 12 (a). Similar tendency was observed for shear failure type specimens, including C14R90, where the anchor side was rotated 90 degrees with respect to the loading direction, as shown in Figs. 12 (b) and (c).

Comparison between C10 and C11 in Fig. 12 (d) shows some differences on the strain development, mainly due to the anchor length, but they appear not to be related with the different concrete strength.

From Fig. 12 (e), it could be observed that the lateral reinforcement ratio increment produces a decrease of the stresses. The lateral reinforcement of specimens C10 (Fc=36N/mm^2) and C11 (Fc=45N/mm^2) did not yielded because of the relatively low concrete strength. On the other hand for specimens C13 (Fc=60N/mm^2) and C14 (Fc=60N/mm^2), the lateral reinforcement did not yielded because of the relatively high lateral reinforcement ratio used for them.

(b) Strain at Anchor End Side

The strain distribution of lateral reinforcement at the anchor end side is shown in Fig. 13. In all cases the strains are small at the end of the anchor, becoming progressively bigger at the start of the bent and at the center of the column. Also as it is shown in the Figs. 13 (a) and (b), there are no differences between specimens with welded closed type hoops and double anchorage type hoops.

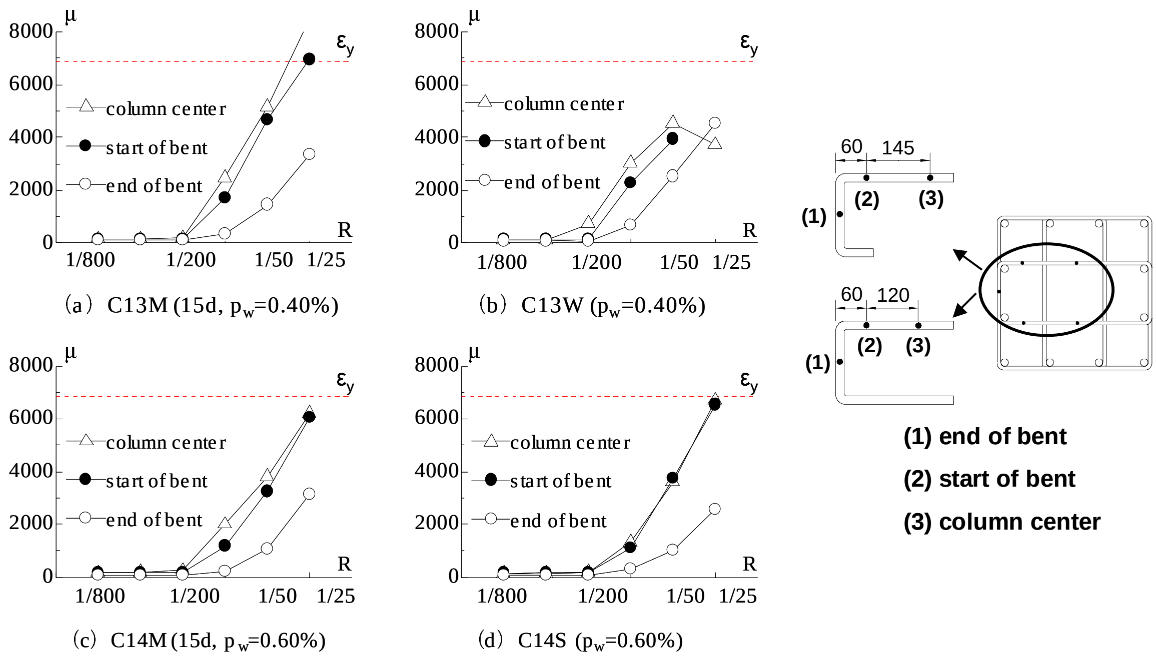

(a) C13M (15d, p_w=0.40%)

(b) C13W (p_w=0.40%)

(c) C14M (15d, p_w=0.60%)

(d) C14S (p_w=0.60%)

Fig. 13 Strain of lateral reinforcement

For specimen C13W with welded closed type hoops, at R=1/25 the strains at the center of the column showed a tendency to become smaller, because the strain gauges which were attached near the welding may have affected the steel deformation properties. For specimens with double anchorage hoops, when a anchor length of 12d (d: bar diameter) is assured, they showed similar behavior compared to the specimens provided with welded closed type hoops as it is understood from Figs. 13(c) and (d).

Contribution of the lateral reinforcement to the shear resistance

The shear strength based on ultimate strength concepts can be calculated by equation proposed by AIJ, as is shown by Eq. (2). This equation is based on the truss arch model theory in structural mechanics wherein the first term is the one contributed by the truss mechanism, while the second term by the arch mechanism.

$$V_u = V_t + V_a = b\, j_t\, p_w\, \sigma_{wy} \cot\phi + \tan\theta (1-\beta) b D \nu \sigma_B / 2 \qquad (2)$$

where:

$$\tan\theta = \sqrt{(L/D)^2 + 1} - L/D \qquad (3)$$

$$\beta = [(1+\cot^2\phi) p_w \sigma_{wy}]/(\nu \sigma_B) \qquad (4)$$

σ_B: Concrete strength

σ_{wy}: Yield stress of the lateral reinforcement (in case of $\sigma_{wy} > 25\sigma_B$ then $\sigma_{wy} = 25\sigma_B$)

b: Column width

j_t : Distance between the centroid of main bars

θ: Angle of concrete compressive strut in the arch mechanism
D: Column depth
L: Clear span
p_w: Lateral reinforcement ratio
$cot\ \Phi$: Angle of the concrete strut in the truss mechanism (cot Φ= 2.0)
ν: Concrete strength effectiveness factor ($\nu = 0.7 - \sigma_B / 196$)

Based on empirical results, it is assumed that for lateral reinforcement having material strength grater than 390MPa and having a yield strength exceeding 25 times the compressive strength, the value for σ_{wy} should be replaced by $25\sigma_B$.

As it can be understood from Eq (2), as much as $p_w\sigma_{wy}$ increases, the factor β also increases, then the second term in Eq. (2), which represents the arch contribution to the shear force, become smaller. Thus as much as $p_w\sigma_{wy}$ increases the tendency is that the shear force will be resisted mainly by the truss mechanism. Also, since the truss and arch model theory is used as shear resisting mechanism, it is assumed that the total diagonal compressive stress in the concrete reaches its effective compressive strength and the stress in the lateral reinforcement also reaches its yield point or its effective value.

For shear failure type specimens, introducing the average strain $\bar{\varepsilon}_w$ (obtained by the strain gauges placed on four layers of hoops on the position denoted as (3) in Fig. 13) in Eq.(5), it is possible to obtain the component of the total shear resistant force carried by the truss mechanism (V_t). Then the arch mechanism component (V_a) to the shear resistance can be calculated by subtracting the truss mechanism component (V_t) from the total shear strength (V_u), which is in this case the experimental value.

$$\sigma_w = E\,\bar{\varepsilon}_w \quad (\sigma_w \le \sigma_{wy}) \tag{5}$$

σ_w: Stress of the lateral reinforcement
$\bar{\varepsilon}_w$: Strain of the lateral reinforcement (average value)

The contribution of the arch and truss mechanism to the shear resistance for specimens with concrete strength of Fc=60N/mm^2, when the lateral reinforcement ratio is varied, is shown in Fig. 14. Up to R=1/200, specimens C12M, C13M and C14M presented few cracks, thus the shear force is mainly resisted by the concrete tensile strength and the arch mechanism. At this stage the truss mechanism did not contribute significantly to the shear resistance, as shown in Fig. 14.

Since R=1/100 as a consequence of the increase of the cracks and concrete deterioration, the stresses of the lateral reinforcement become bigger, and the contribution of the truss mechanism suddenly rises, following a gradually decrease of the contribution of the arch mechanism.

According to the increase of the lateral reinforcement ratio (p_w), up to R=1/50 the contribution of truss mechanism did not present any substantial changes. On the other hand as p_w was increased the ultimate shear strength increased, improving the capability to sustain large deformations without strength decay as shown the in Figs. 14 (a) to (c).

In case of C14 with the biggest p_w, even at R=1/50 the arch mechanism was still contributing to the shear resistance. Thus, it is possible to realize that the concrete core was very well confined at this point. At R=1/25, the resistance mechanism came to be fully transferred to truss mechanism as shown in Fig. 14 (b).

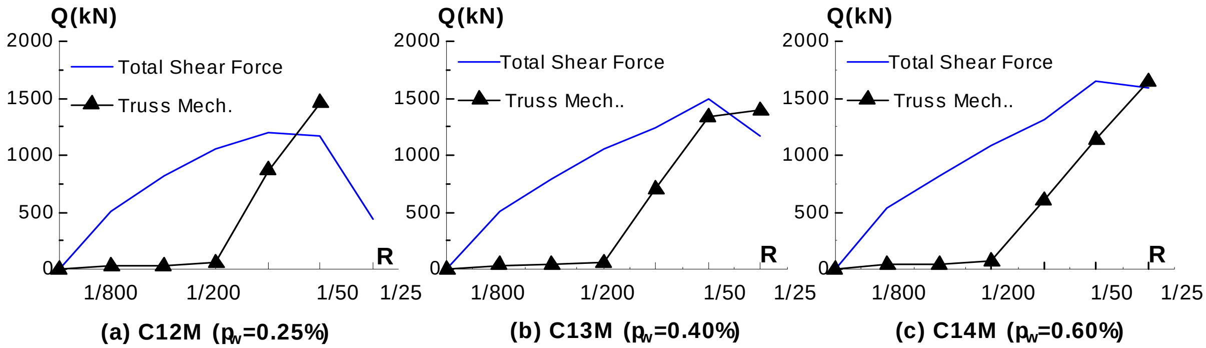

Fig. 14 Components of shear resistance

The relationships of actual concrete strength σ_B to lateral reinforcement ratio p_w and lateral reinforcement stress σ_w are shown in Fig. 15. For specimens with lower σ_B (24 and 36 N/mm^2), either for welded closed type or double anchorage, the ratio σ_w / σ_B varies between 25 and 35, as shown in Fig. 15 (a). This is mainly because of the small lateral reinforcement ratio (0.16%, 0.21%) used for the specimens.

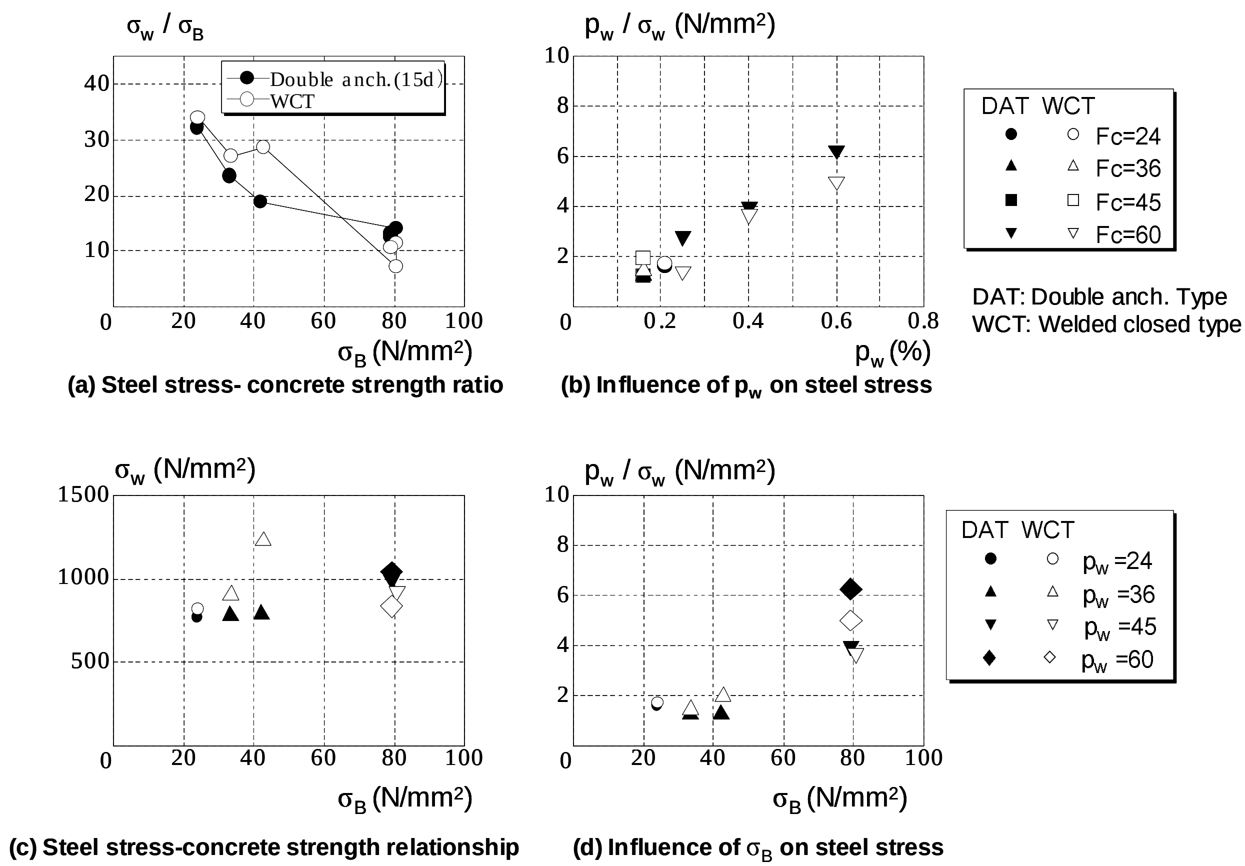

Fig. 15 Concrete strength to lateral reinforcement ratio relationship

When the concrete strength is increased, the lateral reinforcement stresses become slightly higher as shown in Fig. 15(c). However, for specimens with comparable p_w, when the influence of p_w is considered, the lateral reinforcement stresses $p_w\sigma_w$ showed no remarkable increment as shown in Fig. 15 (d). Therefore increasing the concrete strength does not necessarily lead to an increment of the lateral reinforcement stresses, since the super high strength lateral reinforcement presents some limitations in terms of contribution to the shear strength. In accordance to this the Ultimate Strength Design Regulations of AIJ in Japan restrict the use of lateral reinforcement strength to $25\sigma_B$ at maximum.

CONCLUSIONS

Using super high strength bars USD1275 (σ_y=1275 N/mm^2) for double anchorage type hoops as lateral reinforcement of columns the following conclusions can be dawn.

1) Bending failure mode

- Specimens reinforced by double anchor type hoops with an anchor length of 40mm (6d) showed similar performance to those reinforced with welded closed type hoops.

2) Shear failure mode

- When the anchor length in the double anchorage type hoops is 40mm (6d), the hoop anchor becomes relaxed and the lateral reinforcement is unable to show a good performance.
- For concrete strength between 36N/mm^2 to 45N/mm^2, the anchor length of 150mm (24d) showed the same performance to that with 100mm (15d).
- For concrete strength of 80N/mm^2 specimen provided with an anchor length of 85mm (12d) showed that enough anchor strength can be attained, and also showed similar behaviour compared with the specimens reinforced with welded closed hoops.
- Specimen with the anchors rotated 90 degrees respect to the loading direction showed no differences compared to the specimen with the anchors placed in the loading direction.

REFERENCES

1. Japanese Architectural Standard Specification (JASS5): Architectural Institute of Japan, 2003, in Japanese.
2. Recommendation for Detailing and Placing of Concrete Reinforcement: Architectural Institute of Japan, 2004, in Japanese.
3. Imai H. et al: A Research on Anchorage Strength of Lateral Reinforcement End. Annual Meeting of the Architectural Institute of Japan, 1999, pp. 537, in Japanese.
4. Building Center of Japan: Design Guidelines of Reinforced Concrete Structures.
5. Architectural Institute of Japan: Design Guidelines for Earthquake Resistant Reinforced Concrete Buildings Based on Ultimate Strength Concepts, 1988, in Japanese.
6. Kaku T. et al: The proposal of equation for bond splitting strength of reinforced concrete members including high strength concrete level. Concrete Research and Technology, Vol. 3, No.1, Jan. 1992, pp.97-108, in Japanese.
7. Imai H., Castro J.J.: Development of hoops with double right angle anchorage for RC columns, paper No. 2473.